Polymeric ionic liquid sorbent coatings in thin film microextraction: Insight into sorbent selectively for pesticides and cannabinoids

Victoria R. Zeger,[1] David S. Bell,[2] and Jared L. Anderson[1,*]
[1] *Department of Chemistry, Iowa State University, Ames, Iowa 50011 USA*
[2] *Restek Corporation, 110 Benner Circle, Bellefonte, Pennsylvania 16823, USA*

Abstract

Polymeric ionic liquid (PIL) sorbent coatings consisting of polymerizable cations and anions were employed as sorbent coatings in thin film microextraction (TFME) for the extraction of pesticides and cannabinoids. The blades consisted of a thin film of PIL sorbents chemically bonded to vinyltrimethoxysilane-functionalized nitinol sheets. The imidazolium- or ammonium-based PIL sorbents contained aromatic benzyl moieties as well as polar hydroxyl groups or aliphatic functional groups within the chemical structure of the IL monomer. The chemical structure of the IL crosslinkers of the PILs were kept constant across each sorbent, except for the anion, which consisted of either bis[(trifluoromethyl)sulfonyl]imide ([NTf_2^-]), p-styrenesulfonate ([SS^-]), or 3-sulfopropyl acrylate ([SPA^-]). Temperature, salt content, and methanol content were optimized as extraction conditions to maximize pesticide-cannabinoid selectivity using Doehlert design of experiments (DOE). Effects of these three factors on selectivity and extraction efficiency are discussed. The optimal extraction conditions consisting of sample temperature (31 °C), sodium chloride (30% w/v), and methanol content (0.25% v/v) are compared to initial sorbent screening conditions at a sample temperature of 40 °C, 15% (w/v) sodium chloride, and 2.5% (v/v) methanol content. PIL sorbent swelling behavior at different salt and methanol content conditions and its effect on extraction efficiency are hypothesized. Selectivity factors for the sorbents indicated that aromatic moieties within the IL monomer may enhance pesticide-cannabinoid selectivity under optimized conditions, but the extraction efficiency of pesticides that are known to coelute with cannabinoids in the chromatographic separation may be enhanced by employing sorbent coatings with [SPA^-] anions.

Corresponding Author:
Jared L. Anderson
Department of Chemistry
Iowa State University
1605 Gilman Hall
Ames, IA 50011
Tel.: +1 515-294-8356
E-mail address: andersoj@iastate.edu

Keywords: Thin film microextraction; Pesticides; Cannabinoids; Polymeric Ionic Liquids; Selectivity

1. Introduction

Pesticides are often tested as part of quality control testing for consumer products. Acute and/or chronic exposure to pesticides can lead to serious health concerns, including cancer and organ failure. The health and environmental implications of pesticide exposure are explicitly detailed in a review by Sharma et al. [1]. To protect public health, pesticide usage is heavily regulated, requiring testing methods to reach down to low ppb levels [2]. A regularly used technique for pesticide analysis, known as QuEChERS (Quick, Easy, Cheap, Effective, Rugged, and Safe), employs an initial liquid-liquid extraction (LLE) step followed by a sample clean up step [3]. Within the first step of this multi-step process, additional hydrophobic molecules are often extracted along with analytes of interest. If not removed within the second step, high-cost mass spectrometers are required to selectively detect the pesticides of interest [4]. Additionally, a reconcentration step may be necessary to reach desirable detectable limits, which can result in loss of analytes [5]. The application of this method for pesticide testing of cannabis/hemp products is bottlenecked by the high cannabinoid content compared to the trace levels of pesticides; therefore, a pesticide selective method capable of preconcentrating these analytes is preferred.

Alternative methods, such as solid-phase microextraction (SPME), have been explored to extract pesticides from a wide range of matrices, including blood plasma, food products, and soil composites [6–9]. SPME combines both an extraction step and preconcentration step into a single process and can be interfaced with different chromatographic systems [10]. The sorbent coatings used in SPME can also be tuned to better extract analytes of interest or to inhibit the extraction of interfering matrix components [11]. A similar methodology known as thin film microextraction (TFME) was recently developed [14] to increase the surface area-to-volume ratio of the sorbent coating. The thin films employed in this geometry allow for faster mass transfer kinetics compared

63 to SPME, providing faster extraction equilibration [15]. Previously, a TFME method to extract
64 pesticides from environmental water samples was developed using polydimethylsiloxane/divinyl
65 benzene (PDMS/DVB) and PDMS/DVB-carbon mesh supported membranes and was compared
66 to a traditional LLE method for pesticide analysis [16]. Significantly more pesticides were detected
67 using the TFME method with a similar level of accuracy.

68 Custom sorbent coatings have been applied in both SPME and TFME methodologies to
69 extract a wide array of analytes ranging from nucleic acids to volatile organic compounds [17–20].
70 Polymeric ionic liquid (PIL) sorbent coatings were first employed in SPME in 2008 [21]. PILs
71 consist of reactive IL monomers, which result in polymers possessing IL motifs upon
72 polymerization. The unique tunability of IL materials makes them ideal for designing analyte
73 selective sorbent coatings. However, the multitude of possible interaction types between PILs and
74 different analytes creates challenges in fully understanding their extraction behavior in an effort to
75 predict and manipulate their selectivity.

76 A number of studies have demonstrated the influence that salt can have on various
77 polyelectrolyte films [28–31]. Cationic polyelectrolytes, which are polymers containing a cationic
78 backbone, are known to collapse in aqueous solutions with a high salt content and swell under salt-
79 free conditions [28]. Zwitterionic polyelectrolytes contain both an anionic and cationic component
80 within the chemical structure of the monomeric unit, and are known to ion pair with their
81 counterpart in salt-free solutions, but swell in solutions with high salt content [29]. It has also been
82 demonstrated that this swelling behavior can influence adsorption and mass transfer kinetics of
83 analytes into these films [29,32–34]. A similar behavior was thought to influence the partitioning
84 of analytes into PIL sorbent coatings [35]. The complex behavior of polyelectrolytes in various

salt solutions suggests that other sample conditions (i.e., temperature, pH, and organic modifier) may alter an ionic sorbent's ability to extract analytes.

This study aims to understand factors that influence pesticide-cannabinoid selectivity with PIL sorbent coatings for future use in extraction methodologies. Selectivity factors were determined for five sorbent coatings based on partition coefficients obtained under the same extraction conditions. Four out of the five PIL sorbent coatings applied in the TFME methodology consisted of polymerizable cations and anions in both the IL monomer and crosslinker chemical structures. The fifth PIL sorbent coating contained a combination of polymerizable and freely mobile anions to examine if freely mobile anions aid in pesticide-cannabinoid selectivity when compared under similar extraction conditions. The effects of various extraction conditions and the chemical composition of PIL sorbent coatings on pesticide-cannabinoid selectivity are assessed. It was observed that sorbents containing the highest amount of aromatic moieties in the IL monomer provided the highest pesticide-cannabinoid selectivity. This suggests that zwitterionic-like PIL sorbents containing IL monomers with multiple aromatic moieties should be used to achieve better pesticide-cannabinoid selectivity under high salt conditions. These results differ from previous observations, which suggested that aromatic moieties favored the extraction of neutral cannabinoids from salt-free samples; however, these results align with the notion that salt significantly influences the selectivity of ionic sorbent coatings.

2. Materials and Methods

2.1 Reagents and Materials

Imidazole (≥99%), acrylonitrile (≥99%), 4-vinylbenzyl chloride (90%), 1-vinylimidazole (≥99%), 1-benzylimidazole (99%), 1-bromooctane (99%), 3-sulfopropyl acrylate potassium salt, acetonitrile (≥99.9%), triethylene glycol monomethyl ether (m-PEG-3) (≥97.0%),

vinyltrimethoxysilane (VTMS) (98%), and 2-hydroxyl-2-methylpropiophenone (DAROCUR 1173) (>96%) were obtained from Sigma-Aldrich (St. Louis, MO, USA). Chloroform (99.8%), dichloromethane (DCM) (99.5%), methanol (99.9%), ethyl acetate (99.5%), sodium hydroxide (95-100.5%), dimethyl sulfoxide (≥99.7%), hydrogen peroxide (30% aqueous solution), and sodium chloride (NaCl) (≥99%) were obtained from Fisher Scientific (Waltham, MA, USA). Sodium 4-vinylbenzenesulfonate or sodium p-styrenesulfonate ([SS^-]), 1H-benzo[d]imidazole (98%), and triethanolamine (99%) (90%) were purchased from Oakwood Chemical (Estill, SC, USA). Reagents including 1,12-dibromododecane (98%) from Alfa Aesar (Tewksbury, MA, USA), lithium bis[(trifluoromethyl)sulfonyl]imide ($LiNTf_2$)(>98%) from Tokyo Chemical Industry (TCI) (Tokyo, Japan), 2,6-di-tert-butyl-4-methylphenol (BHT) (99.8%) from Acros Organics (Pittsburgh, PA, USA), 1-octylimidazole (>98%) from Ionic Liquid Technologies (IoLiTEC) GmbH (Heilbronn, Germany), and methane sulfonyl chloride (98%) from ThermoScientific (Waltham, MA, USA) were also used. For the TFME blades, nitinol (NiTi) sheet metal (4 in x 0.3 mm x 8 in) was obtained from Nexmetal Corporation (Sheridan, WY, USA). Cannabinoid standards, including cannabidiol (CBD), cannabinol (CBN), cannabigerol (CBG), delta-9-tetrahydrocannabinol (Δ^9-THC), delta-8-tetrahydrocannabinol (Δ^8-THC), and cannabichromene (CBC), as well as all six of the Oregon Pesticide Standards (59 pesticides) were provided by Restek Corporation (Bellefonte, PA, USA). A working solution for the cannabinoids in methanol and a separate working solution for the pesticides in acetonitrile were both made at an analyte concentration of 100 mg L^{-1}. The sample matrix consisted of Type I water (18.2 MΩ·cm) from a MilliQ system (MilliporeSigma, Burlington, MA, USA) since homogenization of dried cannabis plant material in water is required prior to extraction.

2.2 Instrumentation

To confirm the synthesis and purity of newly synthesized IL monomers and crosslinkers, ^{1}H NMR spectra were acquired using either a Varian MR-400 MHz nuclear magnetic resonance (NMR) spectrometer (Palo Alto, CA, USA) or an Avance NEO 400 MHz system with LN2-cooled broadband Prodigy Probe from Bruker Corporation (Billerica, MA, USA). The samples for NMR were prepared in either deuterated dimethyl sulfoxide or deuterium oxide, both from Acros Organics. To polymerize the sorbent coatings, a Rayonet photochemical reactor (RPR-100) from Southern New England Ultraviolet Company (Brandford, CT, USA) was operated at 350 nm.

Two Agilent Technologies (Santa Clara, CA, USA) 1260 Infinity HPLC systems with a 20 µL manual injector were independently used to separate cannabinoids and pesticides. The cannabinoids were detected using a variable wavelength detector at 228 nm, while the pesticides were detected using a diode array detector at 215, 230, and 280 nm. A Restek Raptor ARC-18 column (150 mm x 4.6 mm, 5 µm) and a Restek Raptor biphenyl column (150 mm x 4.6 mm, 5 µm) were used for the separation of cannabinoids and pesticides, respectively, along with a guard cartridge (5 mm x 4.6 mm I.D.) with identical packing to the analytical column. These separations were carried out at 1.0 mL min^{-1} in reverse phase mode using either water and acetonitrile (ARC-18) or water and methanol (Biphenyl), as described previously [36]. Chromatograms are shown in Figures S1-2 of the Supplemental Information (SI). Analyte information including abbreviations, retention times, and detection wavelengths are in Table S1.

2.3 Synthesis of Ionic Liquid Monomers and Crosslinkers

IL monomers and crosslinkers were synthesized according to the procedures described in the literature [35]. Final products were dissolved in a suitable organic solvent (i.e., dichloromethane, ethyl acetate, or acetonitrile) and stored at room temperature in a desiccator. An inhibitor, 2,6-di-tert-butyl-4-methylphenol, was added to all final products for long term stability. When required

for coating, an aliquot of IL solution was portioned off and the solvent removed using an air stream. Table 1 defines the sorbent coating composition for each blade with the names, chemical structures, and abbreviations for the IL monomers and crosslinkers used throughout the manuscript.

2.4 Construction of TFME devices

The NiTi sheet metal was cut into 3 cm by 0.5 cm strips for the TFME blades. The strips were manually etched with sandpaper and rinsed with acetone and water. The NiTi was placed into a 30% aq. hydrogen peroxide solution and refluxed at 72 °C for 2 hours. The NiTi was removed, rinsed with water, and dried using acetone. The metal was covered with VTMS and heated to 85 °C for 3 hours to impart reactive vinyl groups onto the metal surface. The NiTi was removed and cleaned with acetone followed by drying in a vacuum oven overnight. The metal supports were kept in a desiccator until needed.

The surface of the NiTi strips was cleaned with acetone prior to coating. The sorbent coating was weighed out in a 2:1 ratio of monomer-to-crosslinker by mass. DAROCUR 1173, a photoinitiator, was added as 3% by total mass of sorbent coating mixture. To homogenize the monomer and crosslinker and photoinitiator, dichloromethane or acetonitrile (depending on solubilities) was used and then subsequently removed. The sorbent coating mixture was applied to the blades using a glass capillary and polymerized at 350 nm in a photoreactor. Only 2.7 cm of the blade's height was coated to allow the blade to be inserted into the septa of the sample vial cap. The blades were conditioned in methanol prior to use.

2.5 Creation of 3D printed desorption containers

Desorption containers were designed to hold the smallest amount of desorption solvent in an effort to maximize detector response. The length and width of these containers were optimized so that TF blades could easily be inserted into the container without scraping against the sides of the

container. The containers were designed in the likeness of those used by Eitzmann et al. [18]. The containers were created using an UltiMaker S5 3D printer via fused deposition modeling with CPE (a co-polyester material). This material was found to be chemically-resistant to methanol and no background peaks associated with the 3D printed container were observed. The internal dimensions consisted of 2.7 W x 7.5 L x 27 H mm^3 with a 1.0 mm wall thickness. Photos of the desorption container can be found in Figure S3 of the SI.

2.6 Optimization of Extraction Methodology

A 3-factor Doehlert Design of Experiments (DOE) was used to optimize factors that influence analyte solubility in aqueous media – amount of organic solvent, salt content, and temperature of the sample. For percentage of organic solvent, the region of interest spanned from 0-5% (v/v) of methanol. For salt content, the region spanned from 0-30% (w/v) of sodium chloride, and the temperature ranged from 20-60 °C. Extractions of cannabinoids were conducted from a 10 mL aqueous sample containing an analyte concentration of 200 μg L^{-1}; extractions of pesticides were conducted from a 10 mL aqueous sample containing an analyte concentration of 400 μg L^{-1}. The stirring rate was held constant at 600 rpm. Analytes were desorbed into 400 μL of methanol across 25 minutes after being rinsed in 400 μL of DI-water for 1 minute. A central point triplicate was evaluated at the following conditions: 15% (w/v) sodium chloride, 2.5% (v/v) methanol, and 40 °C. Each blade was screened at the central point condition.

Blade **A1** had the highest selectivity values and was used as the model TF blade for optimization of sample conditions. For the DOE, Blade **A1** was used to extract pesticides and Blade **A2** was used to extract cannabinoids. Selectivity values, the response variable, were determined based on the ratio of total peak areas (TPA), or the sum of all peak areas for a class of analytes. The TPA for the pesticides was compared to the TPA of the cannabinoids since the

cannabinoids and pesticides were extracted with two different blades. Regression surfaces and contour plots were generated using R. The R code and statistical evaluation of the model used to construct the response surfaces and contour plots can be found in the SI. Optimal sample conditions consisted of 30 % (w/v) sodium chloride, 0.25% (v/v) methanol, and were equilibrated at a temperature of 31 °C. A 10-minute temperature equilibration time was used. These conditions were used to obtain sorption- and desorption-time profiles.

2.7 Extraction conditions for selectivity determination

The same optimal sample conditions described above were used to obtain the results for calculating selectivity factors. The pesticides and cannabinoids were extracted under the same conditions but from different samples each at an analyte concentration of 400 μg L^{-1}. The TF blades were exposed to the sample for 15 minutes. The blades were then placed into 400 μL of water for 1 minute to rinse off residual salt from the sorbent coatings prior to desorption of the analytes into 400 μL of methanol for 20 minutes.

To accurately quantify the selectivity of each sorbent coating applied to TF blades, selectivity factors (α) were calculated using Eq. 1, considering the ratio of partition coefficients (K_p and K_c):

$$\alpha = \frac{K_p}{K_c} \quad (1)$$

In TFME, partition coefficients compare the concentration of analytes in the sorbent coating to the concentration of analytes remaining in the sample after extraction. Calibration curves were constructed for both sets of analytes to determine the mass extracted by the blades (see Table S4). The sample volume and volume of the sorbent phase were considered constant for both pesticide and cannabinoid extractions since no leaching or disruption of the coating was observed. This further simplifies Eq. 1 down to a ratio of masses (g), as represented by Eq. 2.

$$\alpha = \frac{\frac{g_{p,Blade}}{g_{p,sample}}}{\frac{g_{c,Blade}}{g_{c,sample}}} \quad (2)$$

3. Results and Discussion

3.1 Choice of sorbent coatings

The sorbent coatings employed in this study have been previously utilized to extract pesticides and cannabinoids [35]. These sorbents were designed to be completely polymerizable apart from Sorbent **A**, which contains mobile [NTf_2^-] anions (55% by mol imidazolium ion). The study suggested that sorbent coatings containing hydrogen bond donor moieties and polymerizable anions possess greater affinity for pesticides, meanwhile those containing [NTf_2^-] anions and aromatic moieties or hydrogen bond acceptor moieties have a greater affinity for cannabinoids. Additionally, a linear trend was observed between sorbent affinity and pesticide-cannabinoid selectivity, which suggests that these functionalities would also contribute to differences observed in their selectivity factors. Therefore, a select number of these sorbent coatings were chosen to assess their ability to selectively isolate pesticides from cannabinoids under the same extraction conditions. Sorbents **D** and **E** contain hydrogen bond donor hydroxy groups, aromatic moieties, and different polymerizable anions, and sorbents **G** and **H** contain multiple aromatic moieties along with polymerizable anions. Additionally, sorbent **A** contains aromatic moieties and a mixture of both polymerizable anions and freely mobile [NTf_2^-] anions. These sorbents were used to prepare Blades **D**, **E**, **G**, **H**, and **A**, respectively.

3.2 Precision and batch-to-batch repeatability

As mentioned in section 2.5, sorbent coating selectivity was screened using the central point conditions for the DOE. The selectivity values from these extractions are represented in Figure S4. Blade **A1** exhibited the highest selectivity value followed by **D** = **H** > **E** > **G**; therefore, Blade **A**

was chosen as the model blade for subsequent optimization studies. A 3-factor Doehlert DOE was carried out for both pesticides and cannabinoids, concurrently, using two different blades containing sorbent **A** (Blade **A1** and **A2**). These two blades were prepared at the same time using the same coating mixture, and thus, were made from the same batch of IL monomer and crosslinker. Inter-blade precision was assessed prior to optimization by comparing the extraction efficiency of each blade obtained for cannabinoids at the central point conditions. Extractions were also conducted using the same working solution. As shown in **Figure 1a**, both blades demonstrated similar extraction efficiencies towards the cannabinoids, indicating that these two blades behave similarly. Blade **A1** was used for extracting pesticides and Blade **A2** was used for extracting cannabinoids. Blade **A1** had relative standard deviation (RSD) values ranging from 3.5-7.5% for the cannabinoids and 7.5-19.8% for the pesticides, with 8 pesticides ranging from 7.5-11.8%. Blade **A2** had RSD values ranging from 11.2-14.9% for the cannabinoids. An RSD value equal to or below 15% is considered acceptable for SPME and TFME methodologies [37–39] and indicates good sorbent stability under the extraction and desorption conditions.

A third blade (Blade **A3**) was created containing sorbent **A** and was compared to Blade **A1** and **A2** at the central point extraction conditions. Blade **A3** was created about 6 months after Blade **A1** and **A2** were created using a different batch of the coating mixture. This coating mixture contained a different batch of the IL monomer but was prepared with the same batch of the IL crosslinker. Another ^{1}H NMR spectrum of the IL crosslinker was obtained to ensure that it had not auto-polymerized (see SI). The extractions were also conducted using a different working solution for pesticides and were conducted about 4 months after performing extractions with Blade **A1** and **A2**. The extraction efficiencies of Blade **A3** for both cannabinoids and pesticides are shown in **Figure 1a** and **1b**, respectively. For most analytes, the three blades appeared to perform similarly apart

from CBD, for which Blade **A3** had a lower extraction efficiency compared to Blade **A1** and **A2**. This may be the result of batch-to-batch differences in creating the TF blades. For Blade **A3**, the RSD values ranged from 13.1-19.0% for the cannabinoids and 1.2-17.3% for the pesticides, with only one pesticide being above 15%. Batch-to-batch repeatability is generally accepted to be within 10% [40–43]; however, it is unclear if this value represents the difference between two fabricated devices from the same batch of synthesized material or two batches of synthesized materials. Since only two different batches were compared in this study and RSD values cannot be determined; the inter-blade precision ranged from 3.4-13.9% RSD (n=3) for the cannabinoids. This value represents within batch and between batch variation. Slightly higher peak areas were observed for the cannabinoids when extracted with Blade **A3**. It is plausible that Blade **A3** has a slightly thicker film than Blades **A1** and **A2**, leading to higher average peak areas for CBN, Δ^9-THC, Δ^8-THC, and CBC. Slightly higher average peak areas were also observed for the pesticides under optimized conditions.

3.3 Effect of salt, temperature, and methanol on the extraction of pesticides and cannabinoids

Several parameters were chosen for optimization based on the results of our previous studies [35,36], in which the salt content, methanol content, and sample temperature appeared to have the greatest effect on the extraction of pesticides and cannabinoids. These factors were thought to alter the solubility of analytes in the aqueous sample, and it was shown that these factors can influence pesticide-cannabinoid selectivity [35,36]. Extractions were conducted for each set of analytes with methanol content ranging from 0-5% (v/v), salt content ranging from 0-30% (w/v) sodium chloride, and sample temperature ranging from 20-60 °C. Since salt appeared to previously have the largest effect on pesticide affinity, it was assigned as Factor 2, having the most levels of inquiry

290 (seven). The percentage of organic solvent was assigned as Factor 1, having five levels of inquiry,
291 and sample temperature as Factor 3, having three levels of inquiry. The experimental range for
292 each factor is shown in Table S2 and the design matrix with the associated conditions and
293 responses is shown in Table S3. A multiple linear regression model was generated in R using the
294 rsm package. The code is listed in the SI as well as summary calculations pertaining to the model's
295 suitability in predicting the response variable. The code has the propensity to determine the
296 "optimal" value, known as stationary points. Stationary points exist where the first derivative of a
297 curve equals zero, which can be either a minimum, maximum, or saddle point. The output of the
298 code is based on the nearest stationary point – a local minimum – favoring cannabinoid extraction.
299 The stationary points identified for this model also fall outside the region of interest. When this
300 occurs, it is customarily acceptable to analyze the contour plots and response surfaces to
301 understand where optimal conditions lie within the region of interest [44,45].

302 The response surfaces and 2D contour plots shown in **Figure 2** each depict the behavior of two
303 sample conditions (x- and y- axes) on the selectivity values (z-axis) between pesticides and
304 cannabinoids. **Figure 2a,d** shows the effect of increasing the amount of sodium chloride content
305 in the sample as the sample temperature is adjusted. The selectivity value increased as the salt
306 content was increased and decreased slightly at higher temperatures. The optimal value for the salt
307 content was determined to be 30% (w/v) of sodium chloride. Based on the contour plot, a
308 maximum appears to form at this high salt content when the temperature is just above 30 °C.
309 **Figure 2b,e** shows the effect of increasing the methanol content as the sample temperature was
310 adjusted. Pesticide selectivity is favored when the methanol content and sample temperatures are
311 both low. Based on the contour plot, a maximum exists near 0.5% (v/v) methanol content and just
312 above 30 °C. Based on this plot, the previous plot, and the effective temperature achievable from

313 the hotplate setup used in this work, the optimal temperature was determined to be 31 °C. Lastly,
314 **Figure 2c,f** shows the effect of increasing the methanol content as the salt content is adjusted. At
315 low salt content, the effect of methanol is minor with slightly higher selectivity values observed at
316 higher methanol content. However, at high salt content, the effect of methanol is more pronounced
317 with pesticide selectivity being favored when the methanol content is zero. This can also be
318 observed in the contour plot. For this reason, the methanol content was chosen to be 0.25% (v/v)
319 as a compromise between 0% and 0.5% (v/v).

320 Based on the nature of the DOE's design matrix, individual runs can be plotted, in which one
321 or more factors are held constant, to provide further insight into how these parameters affect certain
322 analytes. These graphs are shown in Figures S5 and S6. In Figure S5, the methanol content was
323 varied as the salt and temperature conditions were kept constant at 15% (w/v) sodium chloride
324 content and 40 °C, respectively. For most pesticides, the peak areas at 0% (v/v) methanol and 2.5%
325 (v/v) methanol were similar, but the peak areas decreased for almost all pesticides at a methanol
326 content of 5% (v/v). Interestingly, a larger relative decrease was observed for later eluting
327 pesticides compared to earlier eluting pesticides. Alternatively, for the cannabinoids, an opposite
328 trend was observed. In this case, as the percentage of methanol increased within the sample,
329 increased peak areas for all cannabinoids were observed, and may possibly be due to the improved
330 solubility of cannabinoids within the sample, resulting in a higher effective analyte concentration
331 [35]. On the other hand, the presence of methanol in the sample may increase the affinity of
332 pesticides for the aqueous phase, resulting in lower peak areas when extractions were performed
333 at a methanol content of 5% (v/v). Therefore, it is clear that the presence of methanol in the sample
334 mostly hinders pesticide-cannabinoid selectivity.

In Figure S6, the effect of salt on each pesticide and cannabinoid is shown at both high levels of methanol content (3.75% (v/v)) and low methanol content (1.25% (v/v)) when the temperature was held constant at 40 °C. Data obtained at low methanol content is represented by the dashed bars, whereas high methanol content is represented by the solid bars. Most pesticides responded better to higher salt content (27.99% (w/v)) except for pesticide 6, which preferred lower salt content (2.01% (w/v)), and pesticide 1, which exhibited no difference for the two. Under the high salt content condition, a more noticeable effect was observed for extractions conducted at high and low methanol content. The extraction efficiency of all pesticides was higher when extractions were performed from samples containing lower methanol content. The complete opposite was true for the cannabinoids, which favored low salt content and high methanol content. The effect of salt, however, appears to be much more significant than the effect of methanol on extraction efficiencies for both pesticides and cannabinoids. It is also clear that the presence of sodium chloride in the sample greatly aids pesticide-cannabinoid selectivity. The effect of temperature could not be assessed in such a way due to the nature of the experimental design.

3.4 Evaluation of sorption and desorption-time profiles

It has been previously demonstrated that the selectivity of SPME can be further enhanced by choosing an optimal extraction time based on the acquired sorption-time profiles [36]. Different sorption-time profiles may occur based on an analytes' partition coefficient; specifically, analytes with smaller partition coefficients are expected to reach equilibrium more quickly [46]. To observe the effect that analyte sorption kinetics may have on the selectivity of TFME, sorption-time profiles were generated using five time points ranging from 1 minute to 45 minutes and are shown in **Figure 3a**. For pesticides, the sorption-time profiles began to level off at around 15 minutes; however, the sorption-time profiles for the cannabinoids increased linearly up to approximately 45

minutes. By observing the ratio of the total pesticide peak areas to the total cannabinoid peak areas at each time point, greater selectivity values were achieved by choosing lower extraction times within the kinetic region of the sorption time profile. However, better repeatability can be achieved by choosing an extraction time within the equilibrium region of the profile. For these reasons, a 15-minute extraction time was chosen for subsequent studies. Sorption-time profiles for each analyte are also shown in Figures S7-8. All pesticides exhibited a similar profile, and all cannabinoids exhibit a similar profile to themselves. With SPME, equilibration for the cannabinoids was not reached until 60 minutes under salt-free conditions [36]. Based on the sorption-time profiles, it appears that the cannabinoids may have greater affinity for the sorbent than the pesticides, resulting in longer equilibration times.

Multiple extraction conditions including stirring/convection, strength of salting-out effect, and sample temperature can also influence analyte sorption kinetics [47]. Fast stirring, higher temperatures, and strong salting-out effects often lead to more rapid sorption kinetics [46,47]. When extractions of pesticides were conducted from samples containing a 30% (w/v) sodium chloride concentration using imidazolium-based PIL SPME fibers, no difference was observed between the 1 minute and 60 minute extractions [36]. This was thought to be due to the strong salting out effect that sodium chloride ions had on the pesticides and was further demonstrated by reducing the concentration of salt present in the sample. In SPME, the sorption time profile is influenced by the volume of the sorbent coating [47], resulting in equilibration times that are dependent upon the thickness of the coating. To prevent long extraction times, the TFME geometry was introduced by Wilcockson and coworker [14]. Where the high surface area-to-volume ratio allows for a higher sorbent volume to be used without sacrificing extraction time. Interestingly, faster sorption times were obtained with SPME rather than TFME. One difference, perhaps,

between the two extraction methodologies is the 10 °C difference in the sample temperature since higher sample temperatures are known to result in faster extraction times [48].

Desorption conditions generally optimized during TFME method development include the desorption solvent, the solvent volume, and the desorption time. The desorption solvent volume was optimized by optimizing the size of the desorption container to fit the blade without damaging the sorbent coating. This was accomplished at the beginning of the study prior to optimizing the extraction conditions. The optimized desorption container holds around 450 µL of methanol, so 400 µL of methanol was chosen as the optimal solvent volume to account for the volume of the blade when inserted into the container. Desorption-time profiles were generated to ensure that all the pesticides are desorbed from the TF blades. Pesticide desorption profiles are shown in **Figure 3b**. No significant difference in peak areas were observed in comparing 1 minute and 20 minute desorption times. This data is consistent with that observed in our previous SPME study, with complete desorption by methanol achieved within 1 minute [36]. This study also determined methanol to be the better desorption solvent over acetonitrile and acetone for PIL sorbent coatings, and so, methanol was kept as the desorption solvent. Carryover experiments were also performed by executing a second successive desorption step in 400 µL of methanol for 20 minute, regardless of the initial desorption time. A single carryover experiment was conducted for each time point and the resulting peak areas were compared to the initial desorption. As the desorption time was increased, the percentage of carryover decreased even though the peak areas from the initial desorption were similar for each desorption time. This may be explained by a loss of analyte to the walls of the desorption container over time, resulting in a shift of the sorbent-solvent equilibrium. Since carryover was lower for desorption steps performed for 20 minute, it was used as the desorption time for subsequent experiments to determine selectivity factors.

3.5 Selectivity factors

The final selectivity factors are shown in **Figure 4**. No significant differences were observed in the selectivity factors when different cannabinoids were compared for the same pesticide. Therefore, the average selectivity factor (α_p) for one pesticide is shown relative to all neutral cannabinoids (c = 1, 2,…, n) monitored in this study (see Eq. 3).

$$\alpha_p = \sum_{c=1}^{n} \alpha_{cp} \quad (3)$$

The results indicate that better selectivity can be achieved by using Blades **G** and **H**, which contain sorbent coatings featuring multiple aromatic moieties. Blade **D** provided the next best selectivity followed by the VTMS-NiTi, Blade **A**, and lastly Blade **E**.

Interestingly, the aforementioned results appear to contradict the conclusion previously drawn when SPME was used to compare selectivity values for these analytes [35]. Prior data suggested that sorbents with hydrogen bond donor groups and polymerizable anions (i.e., Sorbents **D** and **E**) provide greater selectivity over sorbents containing either aromatic moieties, hydrogen bond acceptor functional groups, and/or freely mobile anions (i.e., Sorbents **A**, **G**, **H**). However, data for the pesticides were collected from samples containing 30% (w/v) sodium chloride while the cannabinoid data were collected from samples containing no salt. It was explained that differences in selectivity could be due to polymer conformational changes between salt-free and concentrated salt solutions [35]. It is believed that zwitterionic sorbent coatings undergo swelling upon exposure to high salt containing aqueous solution and that cationic polymer sorbent coatings collapse under these same conditions [31]. However, the significance of these changes is unknown for PIL sorbents, and the high crosslinking density is expected to mitigate swelling behavior [49]. On the other hand, it may be reasonable to expect that different selectivity will be observed when comparing data obtained under the same high salt conditions than from that obtained from low salt

conditions [50,51]. Hydrogen bonding and π-π type interactions, previously thought to influence selectivity, do not appear to be a dominant factor in extracting cannabinoids from high salt samples. Analysis of the selectivity factors show that IL monomers comprising 3 aromatic moieties (Sorbent **G** and **H**) extract pesticides better than cannabinoids. Blade **D,** containing the aromatic [SS^-] anion, also appears better at selectively extracting pesticides compared to the structurally similar Blade **E** containing the non-aromatic [SPA^-] anion. Blade **A3** containing half polymerizable [SS^-] anions and half exchangeable [NTf_2^-] anions offered similar selectivity factors to Blade **E** despite having different chemical structures for their IL monomers, which also have very different assumed polarities [35].

During the sorbent screening process, the following selectivity order was observed under the central point conditions: Blade **A1** > Blade **D** = **H** > Blade **E** > Blade **G**. This order is surprisingly different from that mentioned above but may be explained by looking at the effect different extraction conditions have on the sorbent coating. Firstly, the effect of different extraction conditions on the analytes' solubilities should remain constant from sample-to-sample as long as the extraction conditions remain constant. In this case, the ranking of blade selectivity factors should not be affected. A possible explanation for this change in selectivity order may be ascertained by examining the original data. Figure S9 shows the TPAs for all blades obtained using the initial central point conditions and the optimized conditions for both cannabinoids and pesticides. For cannabinoids, the blade ranking did not change between initial and optimal conditions, but the overall abundance extracted was reduced 10-fold. For the pesticides, however, significant changes in blade ranking were observed, especially for Blades **G** and **H**. When TPAs at the initial conditions were compared to the TPAs at the optimal conditions for each blade, a few interesting observations can be noticed. Blade **A** had similar TPAs for the pesticides under the

initial extraction conditions as the optimal extraction conditions. It is known that the addition of methanol to aqueous samples can result in desolvation and result in specific ion effects [52,53]. Studies of polyelectrolytes have shown that these materials collapse or coil at lower salt concentration when methanol is added to the solution [54,55]. However, the partial cationic nature of this sorbent should already be in a collapsed state in both the 15% and 30% (w/v) sodium chloride solution [28]. Therefore, this effect on the sorbent coating of Blade **A** may not be significant. The TPA of pesticides extracted by Blade **G**, on the other hand, increased greatly when optimal extraction conditions were used. The sorbent of Blade **G** is considered to be of zwitterionic in nature, and at moderate to high salt content, is expected to swell. However, due to the desolvating effect of methanol in aqueous matrices, it is possible that the sorbent was desolvated enough to favor intra-polymer π-π interactions, hindering the sorbent's ability to interact with the analytes [56]. This may also result in a partial collapse of the sorbent. The same may also be true for Blade **H**. Additionally, the desolvating effect may be more significant for hydrophobic sorbents (i.e., Blades **G** and **H**) than more polar/protic sorbents (i.e., Blades **D** and **E**) since more polar sorbents can be better solvated by water molecules via hydrogen bonding. This may account for the observed differences between the two types of sorbents. In further support of intra-polymer π-π interactions, however, Blade **D** possessing an aromatic moiety in the anion component had a more significant increase in TPA compared to Blade **E** having no aromatic moiety in the anion. Therefore, it is evident that aromatic moieties play a significant role in extracting the monitored pesticides, and this observation was not apparent for the cannabinoids.

Relative selectivity factors were also compared by normalizing the calculated selectivity factors to the Z-score for each blade. Z-score normalization centers the data to zero and reduces the standard deviation to one. By normalizing to the Z-score, pesticides for which sorbents have a

greater affinity become more apparent and can be compared across the different sorbents without having to normalize based on the film thickness. **Figure 5** shows the relative selectivity factors of each pesticide for all blades. Pesticides with positive values were more favored by the sorbent whereas those with negative values were less favored. Later eluting pesticides (i.e., pesticides 5-10) appeared to be more favored by all sorbents, apart from pesticide 9. It has been shown previously that cannabinoids coelute with pesticides 5-8 in this separation method [36]. Interestingly, all sorbents appear to have better selectivity for these pesticides, especially for the sorbent of Blade **G**. This superior relative selectivity is due to the sorbents having higher affinity for these pesticides compared to other pesticides. Pesticides 5 and 7 lack aromatic moieties, while pesticide 8 contains one aromatic moiety with an electron-withdrawing group, and pesticide 6 consists of a conjugated π-system with aromatic moieties. Blade **A3** exhibited a surprisingly higher affinity for pesticides 5 and 7, which have less rigid structures due to the lack of aromatic moieties. This selectivity may be due to the collapsed state of the sorbent inhibiting bulkier analytes from partitioning into the sorbent. Additionally, all zwitterionic-PIL sorbents (i.e., Blades **D**-**E** and **G**-**H**) offered high affinity for pesticide 8, except for the sorbent of Blade **A3,** and a relatively higher affinity for pesticide 6 than Blade **A3**. Finally, sorbents containing the [SPA^-] anion appear to have a greater affinity for pesticide 6 than those containing [SS^-] anions (i.e., Blade **D** and **A3**), even though pesticide 6 contains more aromatic moieties. Blades **G**, **H** and **E** also have a greater affinity for pesticide 7 compared to Blade **D**. Therefore, selectivity of these few pesticides may be enhanced by using [SPA^-] anions even though more aromatic moieties resulted in better pesticide-cannabinoid selectivity overall.

4. Conclusions

Five PIL sorbent coatings were examined to determine factors affecting pesticide-cannabinoid selectivity when applied in the thin-film geometry. The percentage of methanol in the sample, the percentage of sodium chloride in the sample, and the sample temperature were optimized to attain the best pesticide selectivity. It was found that high salt content, low methanol content, and mild heating conditions favored pesticide-cannabinoid selectivity. The effect of salt and methanol on the selectivity is believed to be due to the solubility of analytes in the sample as well as the state of the PIL sorbent. Additionally, at high salt conditions, PIL sorbents are believed to behave similarly to polyelectrolytes due to their ionic nature. For cationic sorbents, the sorbents are expected to be in a collapsed state. For zwitterionic-like sorbents, the sorbents are expected to be in a swelled state, allowing for a higher available surface area and stronger sorbent-analyte interactions. However, at high methanol content, swelled sorbents are expected to become desolvated, which may favor intra-polymer interactions over sorbent-analyte interactions. It is believed that these different behaviors may account for the reversal of selectivity order between initial and optimized conditions. Final selectivity factors were calculated based on partition coefficients, and the results indicated that greater pesticide-cannabinoid selectivity may be due to the sorbents possessing more aromatic moieties within the IL monomer. Finally, the strength of pesticide affinity indicates that these sorbents offer greater preference for pesticides that coelute with cannabinoids during chromatographic separations and are ideal for use in a pesticide-selective extraction methodology. Enhanced extraction efficiencies for these pesticides may be obtained by using the [SPA^-] anion over [SS^-] and [NTf_2^-] anions.

5. Acknowledgements

516 The authors acknowledge partial funding of this work through the Chemical Measurement and
517 Imaging Program at the National Science Foundation (Grant No. CHE-2203891). The authors
518 thank Dr. Bruce Richter for his valuable input and discussions.

6. References

[1] A. Sharma, A. Shukla, K. Attri, M. Kumar, P. Kumar, A. Suttee, G. Singh, R.P. Barnwal, N. Singla, Global trends in pesticides: A looming threat and viable alternatives, Ecotoxicol. Environ. Saf. 201 (2020) 110812. https://doi.org/10.1016/j.ecoenv.2020.110812.

[2] C.B. Craven, N. Wawryk, P. Jiang, Z. Liu, X.-F. Li, Pesticides and trace elements in cannabis: Analytical and environmental challenges and opportunities, J. Environ. Sci. 85 (2019) 82–93. https://doi.org/10.1016/j.jes.2019.04.028.

[3] M. Anastassiades, S.J. Lehotay, D. Štajnbaher, F.J. Schenck, Fast and Easy Multiresidue Method Employing Acetonitrile Extraction/Partitioning and "Dispersive Solid-Phase Extraction" for the Determination of Pesticide Residues in Produce, J. AOAC Int. 86 (2003) 412–431. https://doi.org/10.1093/jaoac/86.2.412.

[4] S.H. Monteiro, S.J. Lehotay, Y. Sapozhnikova, E. Ninga, A.R. Lightfield, High-Throughput Mega-Method for the Analysis of Pesticides, Veterinary Drugs, and Environmental Contaminants by Ultra-High-Performance Liquid Chromatography−Tandem Mass Spectrometry and Robotic Mini-Solid-Phase Extraction Cleanup + Low-Pressure Gas Chromatography−Tandem Mass Spectrometry, Part 1: Beef, J. Agric. Food Chem. 69 (2021) 1159–1168. https://doi.org/10.1021/acs.jafc.0c00710.

[5] O. Kiguchi, T. Kobayashi, K. Saitoh, N. Ogawa, Loss of polychlorinated dibenzo-p-dioxins, polychlorinated dibenzofurans and coplanar polychlorinated biphenyls during nitrogen gas blowdown process for ultra-trace analysis, Anal. Chim. Acta. 546 (2005) 102–111. https://doi.org/10.1016/j.aca.2005.05.019.

[6] N.H. Godage, E. Gionfriddo, Biocompatible SPME coupled to GC/MS for analysis of xenobiotics in blood plasma, J. Chromatogr. B. 1203 (2022) 123308. https://doi.org/10.1016/j.jchromb.2022.123308.

[7] E. Gionfriddo, D. Gruszecka, X. Li, J. Pawliszyn, Direct-immersion SPME in soy milk for pesticide analysis at trace levels by means of a matrix-compatible coating, Talanta. 211 (2020) 120746. https://doi.org/10.1016/j.talanta.2020.120746.

[8] A. Tabibi, M.T. Jafari, High efficient solid-phase microextraction based on a covalent organic framework for determination of trifluralin and chlorpyrifos in water and food samples by GC-CD-IMS, Food Chem. 373 (2022) 131527. https://doi.org/10.1016/j.foodchem.2021.131527.

[9] H. Ghosson, D. Raviglione, M.-V. Salvia, C. Bertrand, Online Headspace-Solid Phase Microextraction-Gas Chromatography-Mass Spectrometry-based untargeted volatile metabolomics for studying emerging complex biopesticides: A proof of concept, Anal. Chim. Acta. 1134 (2020) 58–74. https://doi.org/10.1016/j.aca.2020.08.016.

[10] R.P. Belardi, J.B. Pawliszyn, The Application of Chemically Modified Fused Silica Fibers in the Extraction of Organics from Water Matrix Samples and their Rapid Transfer to Capillary Columns, Water Qual. Res. J. Can. 24 (1989) 179–191. https://doi.org/10.2166/wqrj.1989.010.

[11] T. Górecki, P. Martos, J. Pawliszyn, Strategies for the Analysis of Polar Solvents in Liquid Matrixes, Anal. Chem. 70 (1998) 19–27. https://doi.org/10.1021/ac9703515.

[12] C.L. Arthur, Janusz. Pawliszyn, Solid phase microextraction with thermal desorption using fused silica optical fibers, Anal. Chem. 62 (1990) 2145–2148. https://doi.org/10.1021/ac00218a019.

[13] S. Risticevic, H. Lord, T. Górecki, C.L. Arthur, J. Pawliszyn, Protocol for solid-phase microextraction method development, Nat. Protoc. 5 (2010) 122–139. https://doi.org/10.1038/nprot.2009.179.
[14] J.B. Wilcockson, F.A.P.C. Gobas, Thin-Film Solid-Phase Extraction To Measure Fugacities of Organic Chemicals with Low Volatility in Biological Samples, Environ. Sci. Technol. 35 (2001) 1425–1431. https://doi.org/10.1021/es001561t.
[15] R. Jiang, J. Pawliszyn, Thin-film microextraction offers another geometry for solid-phase microextraction, TrAC Trends Anal. Chem. 39 (2012) 245–253. https://doi.org/10.1016/j.trac.2012.07.005.
[16] H. Piri-Moghadam, E. Gionfriddo, A. Rodriguez-Lafuente, J.J. Grandy, H.L. Lord, T. Obal, J. Pawliszyn, Inter-laboratory validation of a thin film microextraction technique for determination of pesticides in surface water samples, Anal. Chim. Acta. 964 (2017) 74–84. https://doi.org/10.1016/j.aca.2017.02.014.
[17] O. Nacham, K.D. Clark, J.L. Anderson, Extraction and Purification of DNA from Complex Biological Sample Matrices Using Solid-Phase Microextraction Coupled with Real-Time PCR, Anal. Chem. 88 (2016) 7813–7820. https://doi.org/10.1021/acs.analchem.6b01861.
[18] D.R. Eitzmann, M. Varona, J.L. Anderson, Thin Film Microextraction Enables Rapid Isolation and Recovery of DNA for Downstream Amplification Assays, Anal. Chem. 94 (2022) 3677–3684. https://doi.org/10.1021/acs.analchem.1c05380.
[19] I.-Y. Eom, S. Risticevic, J. Pawliszyn, Simultaneous sampling and analysis of indoor air infested with Cimex lectularius L. (Hemiptera: Cimicidae) by solid phase microextraction, thin film microextraction and needle trap device, Anal. Chim. Acta. 716 (2012) 2–10. https://doi.org/10.1016/j.aca.2011.06.010.
[20] X. Song, R. Wang, X. Wang, H. Han, Z. Qiao, X. Sun, W. Ji, An amine-functionalized olefin-linked covalent organic framework used for the solid-phase microextraction of legacy and emerging per- and polyfluoroalkyl substances in fish, J. Hazard. Mater. 423 (2022) 127226. https://doi.org/10.1016/j.jhazmat.2021.127226.
[21] F. Zhao, Y. Meng, J.L. Anderson, Polymeric ionic liquids as selective coatings for the extraction of esters using solid-phase microextraction, J. Chromatogr. A. 1208 (2008) 1–9. https://doi.org/10.1016/j.chroma.2008.08.071.
[22] Y. Meng, J.L. Anderson, Tuning the selectivity of polymeric ionic liquid sorbent coatings for the extraction of polycyclic aromatic hydrocarbons using solid-phase microextraction, J. Chromatogr. A. 1217 (2010) 6143–6152. https://doi.org/10.1016/j.chroma.2010.08.007.
[23] C.M. Graham, Y. Meng, T. Ho, J.L. Anderson, Sorbent coatings for solid-phase microextraction based on mixtures of polymeric ionic liquids: Sample Preparation, J. Sep. Sci. 34 (2011) 340–346. https://doi.org/10.1002/jssc.201000367.
[24] J. Pawliszyn, Handbook of solid phase microextraction, Elsevier e-book, Amsterdam Boston Paris, 2011.
[25] J.B. Pawliszyn, Solid Phase Microextraction: Theory and Practice, WILEY-VCH Incorporated, New York, NY, 1997.
[26] C.L. Arthur, D.W. Potter, K.D. Buchholz, S. Motlagh, J. Pawliszyn, Solid-Phase Microextraction for the Direct Analysis of Water: Theory and Practice, LC GC The Magazine of Separation Sciences. 10 (1992) 656–661.
[27] T. Górecki, X. Yu, J. Pawliszyn, Theory of analyte extraction by selected porous polymer SPME fibres†, The Analyst. 124 (1999) 643–649. https://doi.org/10.1039/a808487d.

[28] R. Kou, J. Zhang, T. Wang, G. Liu, Interactions between Polyelectrolyte Brushes and Hofmeister Ions: Chaotropes versus Kosmotropes, Langmuir. 31 (2015) 10461–10468. https://doi.org/10.1021/acs.langmuir.5b02698.
[29] T. Wang, X. Wang, Y. Long, G. Liu, G. Zhang, Ion-Specific Conformational Behavior of Polyzwitterionic Brushes: Exploiting It for Protein Adsorption/Desorption Control, Langmuir. 29 (2013) 6588–6596. https://doi.org/10.1021/la401069y.
[30] T. Wang, R. Kou, H. Liu, L. Liu, G. Zhang, G. Liu, Anion Specificity of Polyzwitterionic Brushes with Different Carbon Spacer Lengths and Its Application for Controlling Protein Adsorption, Langmuir. 32 (2016) 2698–2707. https://doi.org/10.1021/acs.langmuir.6b00293.
[31] F. Hegaard, R. Biro, K. Ehtiati, E. Thormann, Ion-Specific Antipolyelectrolyte Effect on the Swelling Behavior of Polyzwitterionic Layers, Langmuir. 39 (2023) 1456–1464. https://doi.org/10.1021/acs.langmuir.2c02798.
[32] H.-Y. Chin, D. Wang, D.K. Schwartz, Dynamic Molecular Behavior on Thermoresponsive Polymer Brushes, Macromolecules. 48 (2015) 4562–4571. https://doi.org/10.1021/acs.macromol.5b00729.
[33] Y. Li, X. Feng, Y. Ma, T. Chen, W. Ji, X. Ma, Y. Chen, H. Xu, Temperature and magnetic dual responsive restricted access material for the extraction of malachite green from crucian and shrimp samples, New J. Chem. 44 (2020) 10448–10458. https://doi.org/10.1039/D0NJ00230E.
[34] C. Zhang, X. Chu, Z. Zheng, P. Jia, J. Zhao, Diffusion of Ionic Fluorescent Probes atop Polyelectrolyte Brushes, J. Phys. Chem. B. 115 (2011) 15167–15173. https://doi.org/10.1021/jp204612u.
[35] V.R. Zeger, D.S. Bell, J.L. Anderson, Understanding the influence of polymeric ionic liquid sorbent coating substituents on cannabinoid and pesticide affinity in solid-phase microextraction, J. Chromatogr. A. 1706 (2023) 464222. https://doi.org/10.1016/j.chroma.2023.464222.
[36] V.R. Zeger, D.S. Bell, J.S. Herrington, J.L. Anderson, Selective isolation of pesticides and cannabinoids using polymeric ionic liquid-based sorbent coatings in solid-phase microextraction coupled to high-performance liquid chromatography, J. Chromatogr. A. 1680 (2022) 463416. https://doi.org/10.1016/j.chroma.2022.463416.
[37] N. Riboni, J.W. Trzcinski, F. Bianchi, C. Massera, R. Pinalli, L. Sidisky, E. Dalcanale, M. Careri, Conformationally blocked quinoxaline cavitand as solid-phase microextraction coating for the selective detection of BTEX in air, Anal. Chim. Acta. 905 (2016) 79–84. https://doi.org/10.1016/j.aca.2015.12.005.
[38] N. Riboni, F. Fornari, F. Bianchi, M. Careri, A simple and efficient Solid-Phase Microextraction – Gas Chromatography – Mass Spectrometry method for the determination of fragrance materials at ultra-trace levels in water samples using multi-walled carbon nanotubes as innovative coating, Talanta. 224 (2021) 121891. https://doi.org/10.1016/j.talanta.2020.121891.
[39] S. Marín-San Román, J.M. Carot, I. Sáenz De Urturi, P. Rubio-Bretón, E.P. Pérez-Álvarez, T. Garde-Cerdán, Optimization of thin film-microextraction (TF-SPME) method in order to determine musts volatile compounds, Anal. Chim. Acta. 1226 (2022) 340254. https://doi.org/10.1016/j.aca.2022.340254.
[40] A. Sarafraz-Yazdi, F. Ghaemi, A. Amiri, Comparative study of the sol–gel based solid phase microextraction fibers in extraction of naphthalene, fluorene, anthracene and

phenanthrene from saffron samples extractants, Microchim. Acta. 176 (2012) 317–325. https://doi.org/10.1007/s00604-011-0718-9.
[41] X. Wang, H. Rao, X. Lu, X. Du, Application of sol–gel based octyl-functionalized mesoporous materials coated fiber for solid-phase microextraction, Talanta. 105 (2013) 204–210. https://doi.org/10.1016/j.talanta.2012.11.074.
[42] V. Abbasi, A. Sarafraz-Yazdi, A. Amiri, H. Vatani, Determination of Aromatic Amines Using Solid-Phase Microextraction Based on an Ionic Liquid-Mediated Sol–Gel Technique, J. Chromatogr. Sci. 54 (2016) 677–681. https://doi.org/10.1093/chromsci/bmv195.
[43] A. Sarafraz-Yazdi, A. Amiri, G. Rounaghi, H. Eshtiagh-Hosseini, Determination of non-steroidal anti-inflammatory drugs in water samples by solid-phase microextraction based sol–gel technique using poly(ethylene glycol) grafted multi-walled carbon nanotubes coated fiber, Anal. Chim. Acta. 720 (2012) 134–141. https://doi.org/10.1016/j.aca.2012.01.021.
[44] D.B. Hibbert, Experimental design in chromatography: A tutorial review, J. Chromatogr. B. 910 (2012) 2–13. https://doi.org/10.1016/j.jchromb.2012.01.020.
[45] L.K. Skartland, S.A. Mjøs, B. Grung, Experimental designs for modeling retention patterns and separation efficiency in analysis of fatty acid methyl esters by gas chromatography–mass spectrometry, J. Chromatogr. A. 1218 (2011) 6823–6831. https://doi.org/10.1016/j.chroma.2011.07.077.
[46] J. Dewulf, H.V. Langenhove, M. Everaert, Solid-phase microextraction of volatile organic compounds Estimation of the sorption equilibrium from the Kovfits index, effect of salinity and humic acids and the study of the kinetics by the development of an "agitated/static layer" model, (n.d.).
[47] D. Louch, S. Motlagh, J. Pawliszyn, Dynamics of organic compound extraction from water using liquid-coated fused silica fibers, Anal. Chem. 64 (1992) 1187–1199. https://doi.org/10.1021/ac00034a020.
[48] H.L. Lord, J. Pawliszyn, Method Optimization for the Analysis of Amphetamines in Urine by Solid-Phase Microextraction, Anal. Chem. 69 (1997) 3899–3906. https://doi.org/10.1021/ac970375b.
[49] J. Wu, D. Zhang, L. Zhang, B. Wu, S. Xiao, F. Chen, P. Fan, M. Zhong, J. Tan, Y. Chu, J. Yang, Long-term stability and salt-responsive behavior of polyzwitterionic brushes with cross-linked structure, Prog. Org. Coat. 134 (2019) 153–161. https://doi.org/10.1016/j.porgcoat.2019.04.050.
[50] S. Endo, A. Pfennigsdorff, K.-U. Goss, Salting-Out Effect in Aqueous NaCl Solutions: Trends with Size and Polarity of Solute Molecules, Environ. Sci. Technol. 46 (2012) 1496–1503. https://doi.org/10.1021/es203183z.
[51] S. Sakata, Y. Inoue, K. Ishihara, Molecular Interaction Forces Generated during Protein Adsorption to Well-Defined Polymer Brush Surfaces, Langmuir. 31 (2015) 3108–3114. https://doi.org/10.1021/acs.langmuir.5b00351.
[52] T. Wang, G. Liu, G. Zhang, V.S.J. Craig, Insights into Ion Specificity in Water−Methanol Mixtures via the Reentrant Behavior of Polymer, Langmuir. 28 (2012) 1893−1899. https://doi.org/10.1021/la203979d.
[53] Y. Xu, G. Liu, Amplification of Hofmeister Effect by Alcohols, J. Phys. Chem. B. 118 (2014) 7450–7456. https://doi.org/10.1021/jp504317j.
[54] T. Wang, Y. Long, L. Liu, X. Wang, V.S.J. Craig, G. Zhang, G. Liu, Cation-Specific Conformational Behavior of Polyelectrolyte Brushes: From Aqueous to Nonaqueous Solvent, Langmuir. 30 (2014) 12850–12859. https://doi.org/10.1021/la5033493.

[55] Y. Long, T. Wang, L. Liu, G. Liu, G. Zhang, Ion Specificity at a Low Salt Concentration in Water−Methanol Mixtures Exemplified by a Growth of Polyelectrolyte Multilayer, Langmuir. 29 (2013) 3645–3653. https://doi.org/10.1021/la400035e.
[56] M. Liu, F. Bian, F. Sheng, FTIR study on molecular structure of poly(N-isopropylacrylamide) in mixed solvent of methanol and water, Eur. Polym. J. 41 (2005) 283–291. https://doi.org/10.1016/j.eurpolymj.2004.09.008.

Figure Legends

Figure 1. Extraction efficiencies for cannabinoids (a) and pesticides (b) assessed at the central point (initial) conditions of the DOE using three different blades of the same sorbent coating. Blade **A1** and **A2** were prepared at the same time using the same coating mixture. Blade **A3** was made using a different coating mixture on a different day.

Figure 2. Response surfaces and contour plots generated for optimization of sample temperature, percentage of NaCl (w/v), and percentage of methanol (v/v) in solution. A Doehlert design matrix (see Table S3) was used as the independent variables for the model and the ratio of pesticide total peak area (P TPA) to cannabinoid total peak area (C TPA) was used for the response (dependent) variable (i.e., selectivity values). The data were collected using Blade **A1** for the pesticides and Blade **A2** for the cannabinoids. Plots (a) and (d) were sliced at 40 °C, plots (b) and (e) were sliced at 15 % (w/v) NaCl, and plots (c) and (f) were sliced at 2.5% (v/v) methanol content.

Figure 3. Sorption-time profile based on total peak area (TPA) for pesticides (red) and the cannabinoids (green) is shown on the left y-axis in plot (a). The ratio of TPAs on the right y-axis represents the selectivity at different extraction times. The peak areas obtained for each pesticide using different desorption times are shown in plot (b) and the percent carryover is shown in plot (c). Percent carryover for pesticide 10 at the 20-minute desorption time (∗) could not be calculated due to an interfering unknown peak for that separation.

Figure 4. Average selectivity factors for each blade comparing pesticide partition coefficient to the average cannabinoid coefficient. Data were collected under optimized conditions. Error bars represent the propagated error. NiTi is VTMS functionalized NiTi.

Figure 5. Relative selectivity values obtained after Z-score normalization of the average selectivity factors. The graph shows the preference a sorbent has towards one pesticide over another.

736 **Table 1.** Chemical structures and names of IL monomers and crosslinkers used for each TF
737 blade sorbent coating.

Blade	IL Monomer	IL Crosslinker
A	1-octyl-3-(4-vinylbenzyl)imidazolium p-styrenesulfonate [$VBImC_8^+$][SS^-] 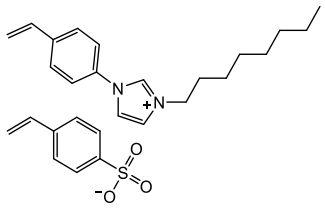	1,12-di(3-vinylbenzylimidazolium)dodecane dibis[(trifluoromethyl)sulfonyl]imide [$(VBIm)_2C_{12}^{+2}$]2[NTf_2^-] 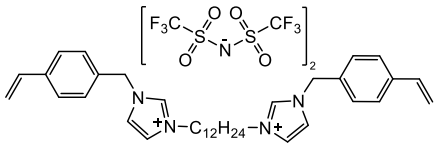
D	N-(4-vinylbenzyl)triethanolammonium p-styrenesulfonate [$VBTOA^+$][SS^-] 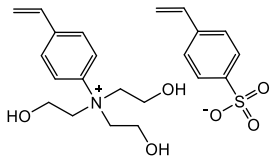	1,12-di(3-vinylbenzylimidazolium)dodecane di[p-styrenesulfonate] [$(VBIm)_2C_{12}^{+2}$]2[SS^-] 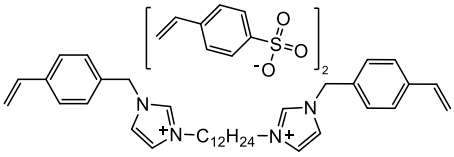
E	N-(4-vinylbenzyl)triethanolammonium 3-sulfopropyl acrylate [$VBTOA^+$][SPA^-] 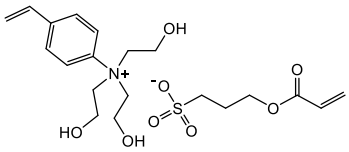	1,12-di(3-vinylbenzylimidazolium)dodecane di[3-sulfopropyl acrylate] [$(VBIm)_2C_{12}^{+2}$]2[SPA^-] 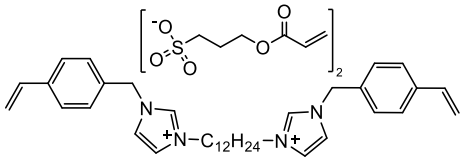
G	1-benzyl-3-(4-vinylbenzyl)imidazolium 3-sulfopropyl acrylate [$VBImBz^+$][SPA^-] 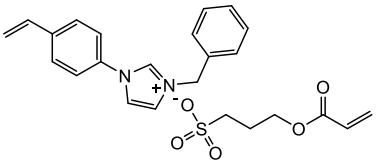	1,12-di(3-vinylbenzylimidazolium)dodecane di[3-sulfopropyl acrylate] [$(VBIm)_2C_{12}^{+2}$]2[SPA^-] 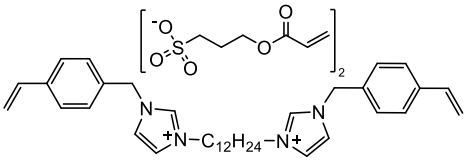
H	1-octyl-3-(4-vinylbenzyl)benzo[d]imidazolium 3-sulfopropyl acrylate [$VBBzImC_8^+$][SPA^-] 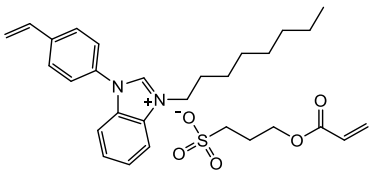	1,12-di(3-vinylbenzylimidazolium)dodecane di[3-sulfopropyl acrylate] [$(VBIm)_2C_{12}^{+2}$]2[SPA^-] 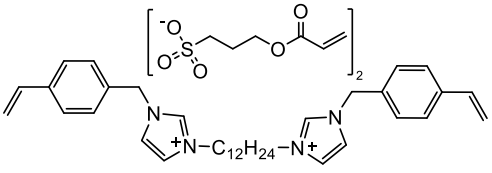
VTMS-NiTi	Vinyltrimethoxysilane (VTMS) 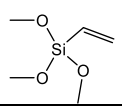	

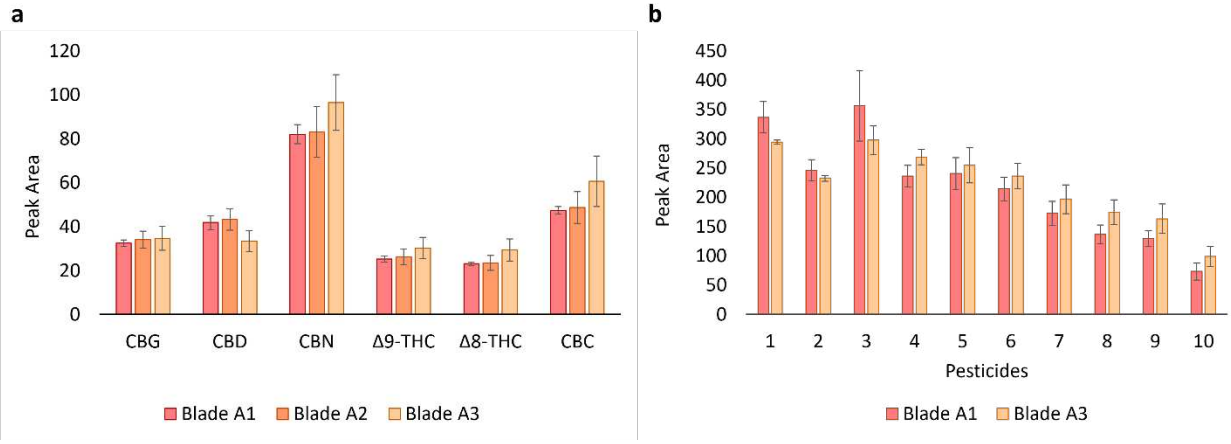

Figure 1. Extraction efficiencies for cannabinoids (a) and pesticides (b) assessed at the central point (initial) conditions of the DOE using three different blades of the same sorbent coating. Blade **A1** and **A2** were prepared at the same time using the same coating mixture. Blade **A3** was made using a different coating mixture on a different day.

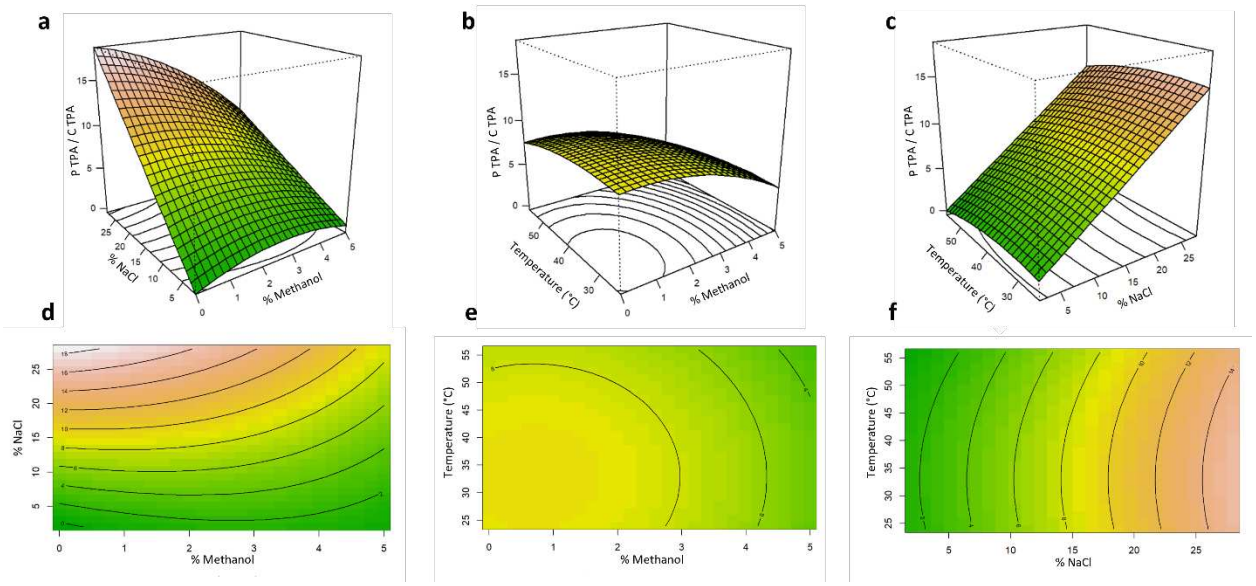

Figure 2. Response surfaces and contour plots generated for optimization of sample temperature, percentage of NaCl (w/v), and percentage of methanol (v/v) in solution. A Doehlert design matrix (see Table S3) was used as the independent variables for the model and the ratio of pesticide total peak area (P TPA) to cannabinoid total peak area (C TPA) was used for the response (dependent) variable (i.e., selectivity values). The data were collected using Blade **A1** for the pesticides and Blade **A2** for the cannabinoids. Plots (a) and (d) were sliced at 40 °C, plots (b) and (e) were sliced at 15 % (w/v) NaCl, and plots (c) and (f) were sliced at 2.5% (v/v) methanol content.

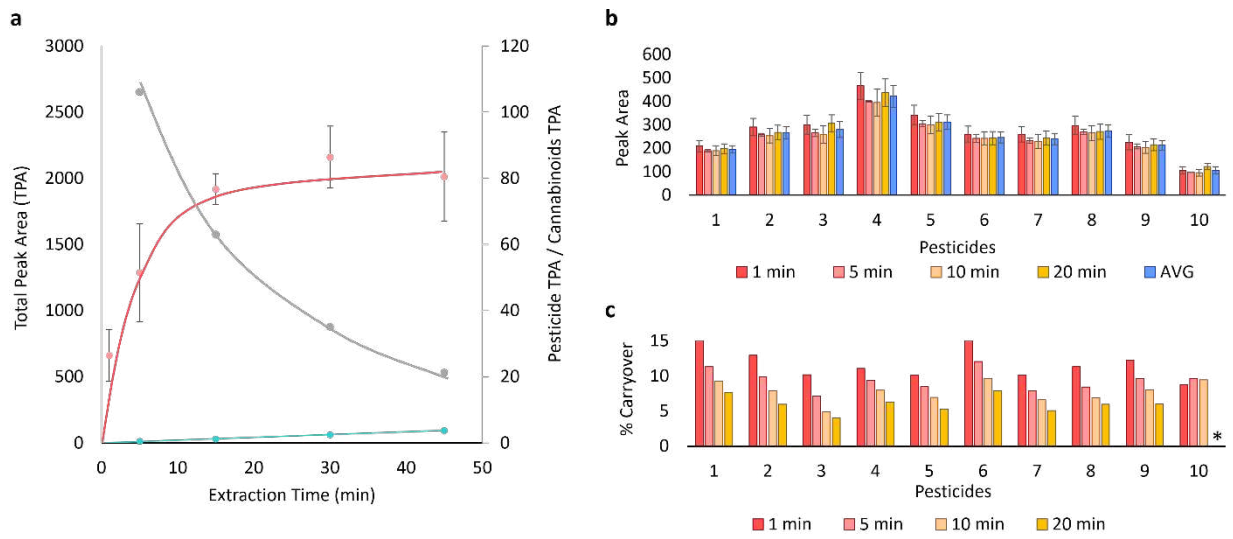

Figure 3. Sorption-time profile based on total peak area (TPA) for pesticides (red) and the cannabinoids (green) is shown on the left y-axis in plot (a). The ratio of TPAs on the right y-axis represents the selectivity at different extraction times. The peak areas obtained for each pesticide using different desorption times are shown in plot (b) and the percent carryover is shown in plot (c). Percent carryover for pesticide 10 at the 20-minute desorption time (*) could not be calculated due to an interfering unknown peak for that separation.

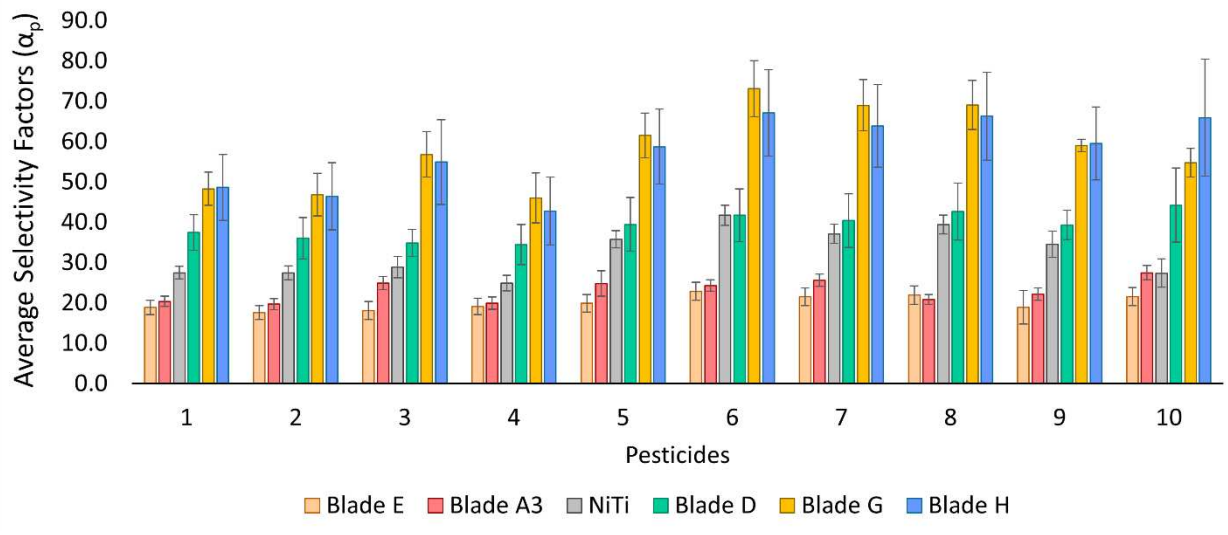

783

784 **Figure 4.** Average selectivity factors for each blade comparing pesticide partition coefficient to
785 the average cannabinoid coefficient. Data were collected under optimized conditions. Error bars
786 represent the propagated error. NiTi is VTMS functionalized NiTi.

787

788

789

790

791

792

793

794

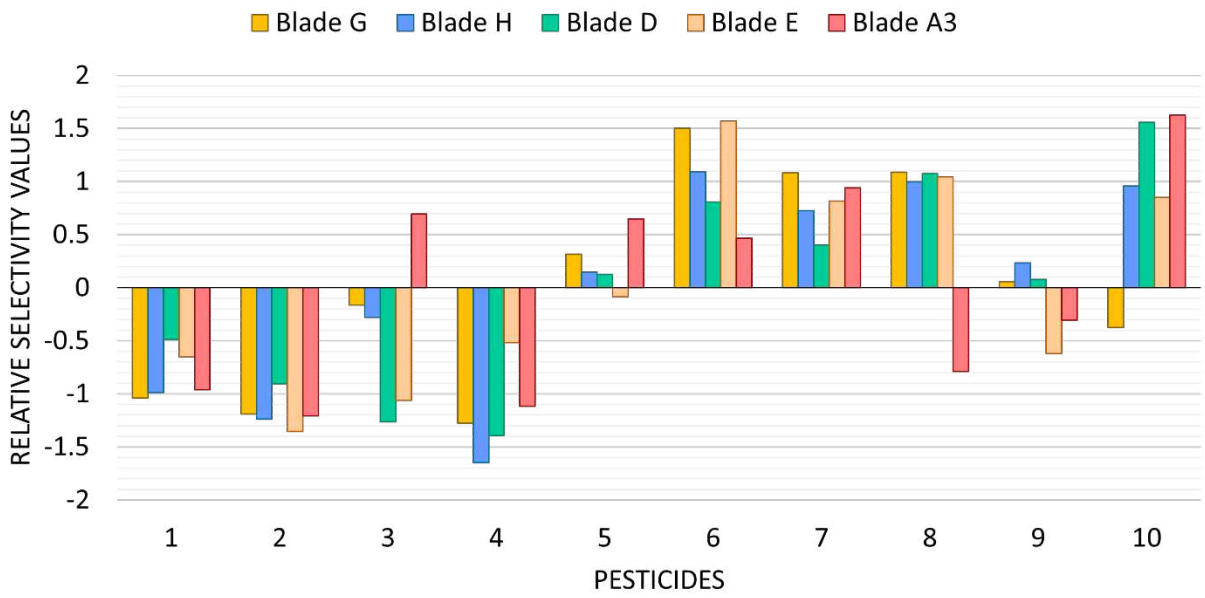

795

796 **Figure 5.** Relative selectivity values obtained after Z-score normalization of the average
797 selectivity factors. The graph shows the preference a sorbent has towards one pesticide over
798 another.